



# Improvement of stomatal resistance and photosynthesis mechanism of Noah-MP-WDDM (v1.42) in simulation of NO<sub>2</sub> dry deposition velocity in forests

Ming Chang<sup>1,★</sup>, Jiachen Cao<sup>1,★</sup>, Qi Zhang<sup>2,3</sup>, Weihua Chen<sup>1</sup>, Guotong Wu<sup>1</sup>, Liping Wu<sup>1</sup>, Weiwen Wang<sup>1</sup>, and Xuemei Wang<sup>1</sup>

<sup>1</sup>Guangdong-Hongkong-Macau Joint Laboratory of Collaborative Innovation for Environmental Quality, Institute for Environmental and Climate Research, Jinan University, Guangzhou, China

<sup>2</sup>School of Atmospheric Sciences, Sun Yat-sen University, Guangzhou, China

<sup>3</sup>Tianjin Academy of Eco-environmental Science, Tjian, China

★These authors contributed equally to this work.

**Correspondence:** Xuemei Wang (eciwxm@jnu.edu.cn)

Received: 13 May 2021 – Discussion started: 1 June 2021

Revised: 3 December 2021 – Accepted: 8 December 2021 – Published: 27 January 2022

**Abstract.** Rapid urbanisation and economic development in China have led to a dramatic increase in nitrogen oxide (NO<sub>2</sub>) emissions, causing serious atmospheric nitrogen pollution and relatively high levels of nitrogen deposition. However, despite the importance of nitrogen deposition, dry deposition processes in forested areas are still insufficiently represented in current global and regional atmospheric chemistry models, which constrains our understanding and prediction of spatial and temporal patterns of nitrogen transport in forest ecosystems in southern China. The offline 1-D community Noah land surface model with multi-parameterisation options (Noah-MP) is coupled with the WRF-Chem dry deposition module (WDDM) and is applied to further understand and identify the key processes that affect forest canopy dry deposition. The canopy stomatal resistance mechanism and the nitrogen-limiting scheme for photosynthesis in Noah-MP-WDDM are modified to improve the simulation of reactive nitrogen oxide dry deposition velocity. This study finds that the combined improved stomatal resistance mechanism and nitrogen-limiting scheme for photosynthesis (BN-23) agree better with the observed NO<sub>2</sub> dry deposition velocity, with the mean bias being reduced by 50.1 %. At the same time, by comparing the different mechanisms of the two processes of canopy stomatal resistance and leaf nitrogen-limiting factors, this study also finds that the diurnal changes in dry deposition velocity simulated by each regional model

present four sets of distributions. This is mainly due to the different ways that each integrated mechanism handles the opening and closing of stomata at noon and the way the nitrogen-limiting factor acts.

## 1 Introduction

Transport and deposition of nitrogen-containing compounds is one of the most critical processes in the study of biogeochemical cycles (Gruber and Galloway, 2008). Atmospheric nitrogen deposition is both the main way that atmospheric reactive nitrogen is removed and an important source of nitrogen for ecosystems (Jefferies and Maron, 1997; Horii et al., 2005). Nitrogen deposition affects changes in the carbon sink in forest ecosystems by affecting plant growth and death (De Vries et al., 2009; Bernhard, 2012). An increase in nitrogen deposition will cause an increase in litter and a decrease in soil decomposition, which will increase the carbon fixation of the soil (Stevens et al., 2004; Liang et al., 2020). Meanwhile, soil acidification caused by nitrogen deposition will reduce the number of microorganisms in the soil, reduce the production of methane, cause the degradation of peatland, and jointly affect the balance of greenhouse gases and the climate (Xu et al., 2009; Cui et al., 2010; Seinfeld and Pandis, 2012; Erisman et al., 2014). At present, studies have shown

that there has been a sharp rise in global and regional atmospheric nitrogen deposition that exceeds the critical load of local ecosystems in many regions (Liu et al., 2013; Yu et al., 2019).

In order to evaluate the impact of atmospheric nitrogen dry deposition on ecosystems, it is important to accurately estimate the dry deposition fluxes of nitrogen components (Wu et al., 2011, 2012; Tian et al., 2018). Scholars calculate the dry deposition velocity of nitrogen-containing components or estimate the effect of variation on dry deposition flux based on global or regional numerical models (Phillips et al., 2006; Zhao et al., 2017; Han et al., 2017; Zhong et al., 2020). The biased results of nitrogen deposition from modelling compared to observations range from  $-70\%$  to  $800\%$  (Chang et al., 2020a). Part of the estimated uncertainty comes from the input bias in the nitrogen emission inventory in the model simulation. For example, Galloway et al. (1994) predicted the nitrogen deposition pattern for 2020, and a large deflection area appeared in an area where emissions did not increase as expected. Another part of the uncertainty comes from the inaccurate simulation of nitrogen concentration. In this situation, the simulated concentration can be verified and nudged by measuring stable oxygen and nitrogen isotope ratios (Guerrieri et al., 2020). At the same time, the simplification and biases of the deposition mechanism in the models compared with satellite retrievals cannot be ignored (Liu et al., 2020). Deposition velocity is difficult to measure and is affected by many coupled physical, chemical and biological processes occurring at the deposition interface.

Therefore, the resistance–velocity method, which is similar to Ohm's law, is used to calculate the dry deposition velocity of various atmospheric species between the atmosphere and the land surface (Szinyei, 2015). In this method, the dry deposition velocity ( $V_d$ ) of gaseous matter is expressed as the reciprocal of the total resistance ( $R_t$ ) of the atmospheric pollutants' deposition process to the land surface. The total resistance is determined by aerodynamic resistance ( $R_a$ ), quasi-laminar boundary layer resistance ( $R_b$ ) and canopy resistance ( $R_c$ ). Their relationship is generally characterised by Eq. (1).

$$V_d = \frac{1}{R_t} = \frac{1}{R_a + R_b + R_c} \quad (1)$$

Here,  $R_a$  is calculated by micrometeorological parameters, which mainly depend on local atmospheric turbulence intensity, while  $R_b$  is driven by the diffusion coefficient and air viscosity of gaseous matter. The calculation of these two resistances in different deposition mechanisms follows similar principles (Finnigan, 2000). At present, the treatment of dry deposition processes affected by turbulent diffusion in numerical models includes two parts: one is the turbulent diffusion process from the bottom of the atmospheric boundary layer to the canopy, and the other is the turbulent exchange process inside the canopy (Flechard et al., 2011, 2013).

The calculation of  $R_a$  is usually based on the turbulent transport part of the land surface model. Most current models are based on the near-surface-layer similarity theory, which first calculates the surface roughness and zero plane displacement and then calculates the turbulent transport coefficient according to the flux gradient relationship under different stratifications (Makar et al., 2017). The calculation of turbulent exchange inside the canopy is more complex and is highly related to the structure of the vegetation canopy and other local properties (Finnigan et al., 2009). Some forest fire models are based on the measured empirical wind speed profiles in the canopy, and other models use the assumption of neutral stratification to solve the turbulent flow fields of the canopy, such as SSiB, SVAT, and BATS (Yongjiu and Qingcun, 1997; Yang and Friedl, 2003; Falge et al., 2005; Moon et al., 2019).

Furthermore, the calculation of  $R_c$  is more complicated and diverse than that of  $R_a$  because  $R_c$  is closely related to differences in the underlying surface, vegetation, soil and other conditions (Wu et al., 2018). Due to differences in the underlying surface,  $R_c$  is usually further decomposed based on canopy type, canopy structure, surface properties of deposition receptors, biochemical reactions of deposition materials, mesophyll uptake and other canopy processes (Ganzeveld et al., 2002; Wolfe and Thornton, 2011; Simpson et al., 2012; Delaria and Cohen, 2020; Massad et al., 2020). For the surface of the vegetation canopy, models are refined to consider the resistance of the stomata, mesophyll, epidermis, soil and other canopy surface factors (Dai et al., 2004; Massad et al., 2020). For example, a multi-layer forest canopy model is used to calculate the canopy stomatal resistance layer by layer at monitoring sites in the Clean Air Status and Trends Network (CASTNET) (Li et al., 2016). As a counterexample, the ocean, which was thought to be a relatively simple surface, has evolved from consideration of smooth levels to sea surface fragmentation, different particle humidities and other factors (Schulz et al., 2012). However, our current understanding of the exchange of nitrogen oxides between the atmosphere and biosphere remains incomplete; Delaria and Cohen (2020) proves the importance of  $\text{NO}_2$  dry deposition and demonstrates that  $\text{NO}_2$  deposition can provide a mechanistic explanation for the canopy reduction of  $\text{NO}_x$ , which has been ignored or unexplained by current common land surface models. For instance, the possible existence of an  $\text{NO}_2$  compensation point toward the leaf surface in forests has been controversial as a result of experimental comparison (Wang et al., 2020). At the same time, the work of Delaria et al. (2018) found that the hypothesis of a nitrogen compensation point may be a problem caused by not adopting a direct  $\text{NO}_2$  measurement technique. The interferences from alkenes or other reactions of biogenic volatile organic compounds may also enhance the observed  $\text{NO}_2$  compensation point and suppress the deposition velocity (Delaria et al., 2018; Place et al., 2020). This will likely lead to changes in our traditional treatment of the parameterisation of nitrogen

exchange in the model. The coupling of canopy photosynthesis, nutrient stress, the impact of mesophilic processes and other plant physiological processes is still poorly resolved in the field of dry deposition model improvement (Massad et al., 2020).

In this study, we apply different improved stomatal resistance mechanisms and nitrogen limitations on photosynthesis mechanisms to the Noah-MP model coupled with dry deposition schemes to explore changes in nutrient stress in stomatal conductance and evaluate the consequences of these changes on NO<sub>2</sub> dry deposition velocity. This paper is organised as follows: following this introductory Sect. 1, Sect. 2 presents a full description of the improved stomatal resistance mechanisms and different schemes of nitrogen limitation of photosynthesis. Section 3 includes model evaluation and discussion about the influence on NO<sub>2</sub> dry deposition velocity simulation, the respective path of canopy stomatal and photosynthesis processes, and the sensitivity of major parameters. Finally, a conclusion and a future research plan for the Noah-MP model and the WRF-Chem dry deposition module (WDDM) framework are summarised in Sect. 4.

## 2 Model description and configuration

### 2.1 Base model setup

This study uses the coupled single-point (1-D) Noah-MP model and the WRF-Chem dry deposition module (WDDM) as its base model (Noah-MP-WDDM, which was developed by Zhang et al., 2017). In order to reduce the effect of meteorological simulation biases on  $V_d$  simulation, the micro-meteorological observation test datasets of Zhang et al. (2017) are used to drive this dry deposition single-point (1-D) Noah-MP-WDDM model and all improvements. However, it is worth noting that when this single-point simulation is upscaled to a regional or global model, it may bring more uncertainty due to the scale conversion. In addition, all the land surface parameters used in this study are the default parameters inside the Noah-MP land surface model's look-up tables (VEGPARM.TBL, SOILPARM.TBL and MPTABLE.TBL). This may cause systematic uncertainties in the overall modelling. The observation data were obtained at the Dinghushan Forest Ecosystem Research Station (Fluxnet site code: CN-Din; 23°10'24" N, 112°32'10" E; altitude 300 m). The NO<sub>2</sub> concentration was measured using the Model T200 (Teledyne-API, USA) NO<sub>2</sub> analyser (Zhang et al., 2017).

Physical processes related to snow, permafrost and other factors – like supercooled liquid water in frozen soil (FRZ), frozen soil permeability (INF), snow surface albedo (ALB), partitioning precipitation into rainfall and snowfall (SNF), lower boundary of soil temperature (TBOT), and snow and soil temperature time scheme (STC) – only have a small effect on  $V_d$  because Dinghushan is located in the subtropics.

Thus, these physical parameterisation schemes all use the default option (Niu, 2011). In contrast, the other six physical parameterisation schemes – dynamic vegetation model (DVEG), canopy stomatal resistance (CRS), soil moisture factor for stomatal resistance ( $\beta$ ) factor (BTR), runoff and groundwater (RUN), surface exchange coefficient for heat (SFC;  $C_H$ ), and radiation transfer (RAD) – have a great influence on  $V_d$  simulation. Their respective options are the dynamic vegetation option (opt\_dveg=2), the Ball–Berry canopy stomatal resistance option (opt\_crs=1), the BATS soil moisture factor option (opt\_btr=3), the original surface and subsurface runoff option (opt\_run=3), the original Noah surface layer drag coefficient option (opt\_sfc=2), and the two streams applied to grid cell radiation transfer option (opt\_rad=2) in the above physical parameterisation schemes (Niu, 2011; Chang et al., 2020b).

### 2.2 Coupling of stomatal resistance schemes

Previous studies have generally used the Jarvis stomatal conductance model, which is based on environmental factors such as photosynthetic effective radiation, temperature, humidity, and soil water to calculate canopy stomatal resistance (Jarvis, 1976). Compared with Jarvis, the Ball–Berry stomatal conductance model (Ball et al., 1987) calculates the stomatal resistance based on the through-canopy photosynthesis rate, CO<sub>2</sub> concentration and humidity on the leaf surface, as shown in Eq. (2). This type of mechanism requires a coupled photosynthesis model to calculate or observe the photosynthesis rate of the canopy, and the photosynthesis model depends on the setting of many plant physiological parameters (optimal photosynthesis efficiency, catalytic enzyme activity parameter  $Q_{10}$ , etc.). It is worth noting that these parameters are often inaccurate at the regional scale, which brings some uncertainty (Dai et al., 2019; Fisher and Koven, 2020).

Although the Ball–Berry type stomatal resistance scheme behaves very similarly to the Jarvis type in modelling transpiration, the former scheme allows a direct coupling of terrestrial water and carbon fluxes and improves the simulation of vegetation–atmosphere interactions (Niyogi et al., 2009; Yang et al., 2011). The Noah-MP model sets the stomatal conductance slope of the Ball–Berry mechanism as a constant, which is not suitable and will cause a large simulation bias. Therefore, we integrate observational experimental results, statistical fitting or plant physiological model equations in photosynthesis, stomatal conductance and other aspects of plant physiology in this study by writing the equation as sub-routines and adding to the calling tree in the coupled single-point Noah-MP-WDDM model.

The calculation equation is Ball et al. (1987) as follows:

$$\frac{1}{R_s} = m \times \frac{A}{C_{\text{air}}} \times \frac{e_{\text{air}}}{e_{\text{sat}}(T_v)} \times P_{\text{air}} + g_{\text{min}}, \quad (2)$$

where  $m$  is the slope of the stomatal conductance,  $A$  is the photosynthetic rate,  $C_{\text{air}}$  is the  $\text{CO}_2$  concentration on the leaf surface,  $e_{\text{air}}$  is the vapour pressure on the leaf surface,  $e_{\text{sat}}(T_v)$  is the saturated vapour pressure of the leaves at the canopy temperature,  $P_{\text{air}}$  is the surface pressure and  $g_{\text{min}}$  is the minimum stomatal conductance.

In addition, the non-stomatal resistance ( $R_{\text{ns}}$ ) calculated in Noah-MP is according to Zhang et al. (2003):

$$\frac{1}{R_{\text{ns}}} = \frac{1}{R_{\text{ac}}} + \frac{1}{R_{\text{cut}}}, \quad (3)$$

where  $R_{\text{ac}}$  is the in-canopy aerodynamic resistance, which is common to all gases, and  $R_g$  and  $R_{\text{cut}}$  are the resistances for the uptake by the ground or soil and canopy cuticle. Similar to the work of Wesely (1989),  $R_g$  and  $R_{\text{cut}}$  are parameterised for  $\text{O}_3$  from look-up tables.

The equations integrated into the single-point mechanism model are shown in Table 1 and are differentiated from each other as follows.

- MBM-1 (modified Ball–Berry mechanism, MBM) is the stomatal conductance equation of the default Ball–Berry equation, and the main parameter used is the slope of the Ball–Berry conductance relationship and the minimum stomatal conductance ( $g_{\text{min}}$ ).
- Leuning (1990) introduced a  $\text{CO}_2$  compensation point  $\Gamma$  to improve the Ball–Berry equation so that it can simulate the net photosynthetic rate and stomatal conductance when the  $\text{CO}_2$  concentration on the blade surface is equal to the compensation point (Table 1, MBM-2). The method of Lohammar et al. (1980) was adopted to replace RH with the water vapour saturation function  $f(D)$ , while its equation has been applied to a variety of plant physiological models (Leuning, 1995) (Table 1, MBM-4).
- Aphalo and Jarvis (1993) separated the effects of temperature and water vapour difference  $D$ , which more directly reflects the effect of temperature on stomatal conductance than the original Ball–Berry equation (Table 1, MBM-3).
- Yu et al. (2004) measured stomatal conductance of wheat under normal atmospheric and artificially increased  $\text{CO}_2$  concentration, as well as the response curve of photosynthesis to light and  $\text{CO}_2$  concentration. Based on this, researchers constructed an equation reflecting the physiological response of plants, which could reflect the relationship between stomatal conductance and photosynthesis rate (Table 1, MBM-5).
- Ye and Yu (2008) derived a model of leaf stomatal mechanism based on experimental observation of light response and stomatal conductance data, which can better simulate the relationship between stomatal conductance and photosynthetic rate (Table 1, MBM-6).

- Medlyn et al. (2011) introduced the optical contract rate coefficient  $g_1$  (Table 1, MBM-7), which led to better simulation results in models such as CABLE (De Kauwe et al., 2015).

## 2.3 Improvements in nitrogen-limiting schemes for photosynthesis

The combination of the DVEG mechanism and the Ball–Berry model can comprehensively consider the interaction between photosynthesis rate and canopy stomatal resistance. This is physiologically significant in that it balances the supply and demand of  $\text{CO}_2$  in the chemical reaction of photosynthesis, which maintains a reasonable concentration of  $\text{CO}_2$  in the mesophyll tissue. However, at the vegetation canopy scale, the photosynthetic rate is also related to the nitrogen content of leaves. Currently, the commonly used biogeochemical models usually express the effect of nitrogen on the photosynthetic process based on the relevant theory of nitrogen limitation, but they often simplify it (Li et al., 2013).

In this study, the original DVEG mechanism of Noah-MP set the nitrogen limitation factor of leaves  $f(\text{N})$  as a function of leaf nitrogen concentration ( $C_{\text{N}}^{\text{leaf}}$ ) and the maximum nitrogen concentration parameters (FOLNMX) of this vegetation type ( $f(\text{N}) = C_{\text{N}}^{\text{leaf}} \cdot \text{FOLNMX}^{-1}$ ). However,  $C_{\text{N}}^{\text{leaf}}$  and FOLNMX were set as two constants, which is obviously an oversimplification for land surface simulation in a large area (Bonan, 1995). For different types of plants, the nitrogen content in leaves should make a significant difference in photosynthetic nitrogen utilisation efficiency (Zheng and Shanguan, 2007). For regional nitrogen deposition simulation, it is obviously inappropriate to simplify the nitrogen-limiting process in leaves, and thus a more accurate description of the effect of nitrogen on plant photosynthesis and a more accurate estimation of the effect of nitrogen deposition on the whole forest ecosystem are needed.

According to whether the nitrogen content of plant tissues is directly taken as the variable in the equation, the current expressions of how nitrogen affects photosynthesis (as shown in Table 2) can be divided into implicit and explicit expressions.

### 2.3.1 Implicit expressions

For the photosynthetic rate model calculated by the Farquhar model (Farquhar et al., 1980), the photosynthetic rate is determined by the minimum value of carboxylation efficiency ( $W_c$ ), carboxylation efficiency ( $W_j$ ) and organophosphorus carboxylation efficiency ( $W_e$ ), which is limited by the concentration of chlorophyll photoenzyme (RuBisCO), in which  $W_c$  and  $W_e$  are proportional to the maximum carboxylation rate ( $V_{\text{cmax}}$ ).

Therefore, the effect of nitrogen on photosynthesis,  $V_{\text{cmax}}$ , is reflected mainly in the limitation of  $f(\text{N})$ . As mentioned above,  $f(\text{N})$  was set by two constants in the DVEG dynamic

**Table 1.** The coupled stomatal conductance and resistance equation lists.

Experiment code	Mechanism equation*	Reference
MBM-1	$g_s = \frac{1}{R_s} = m \times \frac{A}{C_{\text{air}}} \times \frac{e_{\text{air}}}{e_{\text{sat}}(T_v)} \times P_{\text{air}} + g_{\text{min}}$	Ball et al. (1987)
MBM-2	$g_s = g_0 + a \cdot A_n \frac{\text{RH}}{C_s - \Gamma^*}$	Leuning (1990)
MBM-3	$g_s = \frac{A_n \times \text{RH}}{C_s} [k_0 + k_1 \times D + k_2 \times T_1 + k_3 \times T_1 \times D]$	Aphalo and Jarvis (1993)
MBM-4	$g_s = g_0 + a \cdot \frac{A_n}{\left(1 + \frac{D}{D_0}\right) \cdot (C_s - \Gamma^*)}$	Leuning (1995)
MBM-5	$g_s = a \cdot \frac{V_{\text{cmax}} \alpha Q \eta}{V_{\text{cmax}} \alpha Q + V_{\text{cmax}} \eta C_a + \alpha Q \eta C_a} \cdot \frac{1}{1 + \frac{D}{D_0}} \cdot \frac{\psi - \psi_0}{\psi_m - \psi_0}$	Yu et al. (2004)
MBM-6	$g_s = g_0 + \frac{1}{4\eta} \cdot \frac{A_{\text{net}}}{C_a - C_i} \cdot f(\text{RH}, T_L)$	Ye and Yu (2008)
MBM-7	$g_s = g_0 + 1.6 \cdot \left(1 + \frac{g_1 \beta}{\sqrt{D}}\right) \frac{A}{C_s}$	Medlyn et al. (2011)

\* For the symbols in the mechanism equations, please refer to the source literature.

**Table 2.** Nitrogen limit schemes for the photosynthesis mechanism.

Experiment code	Classify	Mechanism equation*	Source models
MNM-1	Implicit	$v_{\text{cm}} = f(\text{N}) \cdot V_{\text{cmax}}$ $f(\text{N}) \in [0, 1]$	Noah-MP, Noah-LSM CLM4.0, AVMIN
MNM-2	Implicit	$v_{\text{cm}} = f(\text{N}) \cdot V_{\text{cmax}}$ $f(\text{N}) = B_L \cdot B_{V_{\text{max}}}$	IBIS, InTEC BEPS, DLEM
MNM-3	Implicit	$\text{GPP} = f_{\text{GPP},\text{N}} \cdot f_{\text{GPP},\text{others}} \cdot \text{GPP}_{\text{max}}$ $f(\text{GPP},\text{N}) = \frac{N_{\text{av}}}{k + N_{\text{av}}}$	Lin et al. (2000)
MNM-4	Implicit	$\text{GPP} = f_{\text{GPP},\text{N}} \cdot f_{\text{GPP},\text{others}} \cdot \text{GPP}_{\text{max}}$ $f(\text{GPP},\text{N}) = \min \left( 1.0, \frac{N_{\text{av}}}{\frac{\text{NPP}_{\text{max}}}{B_{\text{max}}}} \right)$	TRIRLEX, 3-PG
MNM-5	Explicit	$v_{\text{cm}} = \frac{\text{act} \cdot f_{\text{lnr}}}{f_{\text{lnr}} \cdot \text{SLA} \cdot C : N_{\text{leaf}}}$	Biome-BGC
MNM-6	Explicit	$v_{\text{cm}} = \frac{(A_b + R_d [P_c + K_c (1 + \frac{P_0}{K_0})])}{P_c - 0.5 P_0 / \tau}$ $A_b = \frac{190 \cdot n}{360 + n}$	CEVSA, Doly

\* For the symbols in the mechanism equations, please refer to the source literature.

vegetation process mechanism. In addition, models such as AVIM (Ji, 1995), CLM4.0 (Oleson et al., 2010) and Noah-LSM (Bonan, 1995) also directly take  $f(\text{N})$  as a parameter, ranging from 0.5 to 1 (Table 2, MNM-1, MNM standing for modified nitrogen mechanism).

However, BEPS (Liu et al., 1999), DLEM (Tian et al., 2010), IBIS (Liu et al., 2005), InTEC (Chen et al., 2000) and

other models use the ratio of the optimal carbon–nitrogen ratio ( $B_{V_{\text{max}}}$ ) to the simulated actual carbon–nitrogen ratio ( $B_L$ ) to represent  $f(\text{N})$  (Table 2, MNM-2).

Models that calculate photosynthesis processes based on empirical functions (such as CASA, Friedlingstein et al., 1999; Lin, Lin et al., 2000; PnET, Aber and Federer, 1992; TEM, McGuire et al., 1997; TRIPLEX, Peng et al., 2002;

and 3-PG, Landsberg and Waring, 1997) mostly use the form of vegetation productivity, which is proportional to light interception, to calculate the net primary productivity (NPP) or total primary productivity (GPP) of vegetation (Monteith, 1972; Monteith and Moss, 1977). Such models generally use implicit methods to limit GPP or NPP in order to implicitly limit the calculation of photosynthesis rate, thus affecting canopy stomatal conductance (Table 2, MNM-3, MNM-4).

### 2.3.2 Explicit expressions

The explicit method is in direct accordance with plant physiology experiments to establish the relation between the  $V_{cm}$  and  $c_N$  functions, and leaf nitrogen content can be measured more directly in the plant physiology sense in relation to photosynthesis. Different researchers get different function relations, and thus there is no unified explicit expression of the equation.

For example, in Biome-BGC (Thornton et al., 2002),  $V_{cm}$  is calculated by the carbon–nitrogen ratio ( $C : N_{leaf}$ ), the ratio of the RuBisCO enzyme middle nitrogen content to total leaf nitrogen content ( $f_{nr}$ ), specific leaf area index (SLA), etc. (Table 2, MNM-5).

Doly and CEVSA established a functional relationship between light saturation rate ( $A_b$ ) and leaf nitrogen absorption rate ( $n$ ) (Woodward et al., 1995; Cao and Woodward, 1998) (Table 2, MNM-6).

### 2.4 Experiment setup for mechanism comparison

After integrating all the improved equations of the canopy stomatal resistance mechanism and the nitrogen-limiting schemes for photosynthesis into the single-point model in the form of subroutines, an orthogonal experimental scheme was adopted to simulate them, and all the experimental schemes were driven by the same meteorological forcing data. The code names of each simulation experiment are shown in Fig. 2, where the original Noah-MP-WDDM model from Zhang et al. (2017) is named BN-11. Since all the mechanisms can be combined into 42 combinations, the current version number is set at v1.42 in this study.

## 3 Results

### 3.1 Model validation

To evaluate the applicability of the single-point Noah-MP-WDDM dry deposition model and all its improvements, we compared the base model results (BN-11) to the observations of latent heat (LH) and sensible heat (SH) fluxes. Detailed statistics of the comparison are shown in Table 3. It can be seen that the simulation of average SH is overestimated by about  $20 \text{ W m}^{-2}$ , while the average LH is underestimated by about  $0.1 \text{ W m}^{-2}$  compared with observations. The

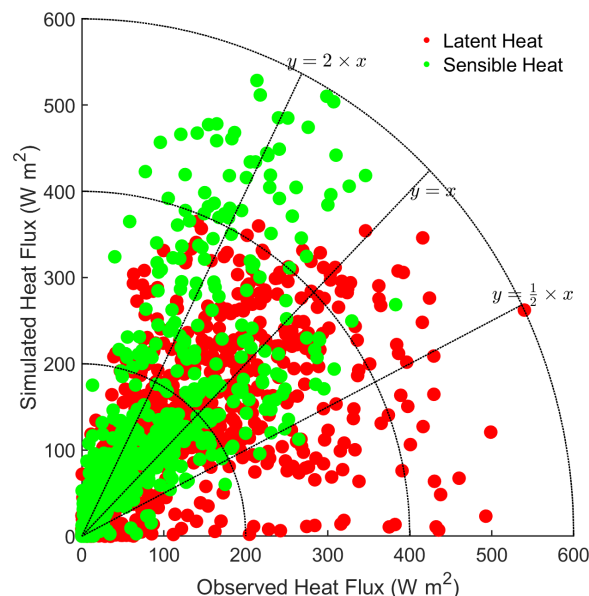


**Figure 1.** Comparison of observed and simulated fluxes of latent heat and sensible heat.

models perform reasonably well for most simulations, with uncertainties within a factor of 0.5–2 (Fig. 1).

### 3.2 Performance of $V_d$ simulation with different mechanisms

The model simulation shows obvious underestimation of  $V_d$ . The simulated average  $V_d$  is about a quarter of the observed results. The correlation coefficient is very low and basically cannot reflect the trend characteristics (Fig. 2). On the one hand, the Noah-MP-WDDM model itself has a poor ability to simulate the change trend of deposition. On the other hand, it is also affected by too much precipitation in subtropical regions, poor quality control of dry deposition observation data and many missing values (Zhang et al., 2017). The observation instrument was limited by the conditions surrounding the flux tower, and the assayed gas had accumulated (especially at night) in the reaction chamber, resulting in a partial (nocturnal) high observed value (Zhang et al., 2017).

It can be seen from Fig. 2 that the simulation effect of each model mechanism is relatively poor, especially for all the combinations corresponding to the MBM-5, MBM-6, MBM-7 and MNM-5 series; the simulated  $V_d$  in these series is basically concentrated around  $0.05 \text{ cm s}^{-1}$ . This indicates that the stability of the parameterisation of these series of mechanisms is relatively high and that the disturbance caused by different schemes in other processes is suppressed.

There is a magnitude difference between the results of the simulation and the observed  $V_d$ , which may be because these mechanisms are not supported with some coniferous species because conifers have little direct stomatal response to elevated  $\text{CO}_2$  (Medlyn et al., 2011; Katul et al., 2012).

**Table 3.** Statistical results of original simulated values and observed values.

Evaluation criteria	Latent heat flux	Sensible heat flux
Mean observation	66.42	29.81
Mean simulation	65.20	48.55
Mean bias	−0.14	20.18
Mean absolute percentage error (MAPE)	2.36	3.12
Root-mean-square error (RMSE)	82.29	60.64
Correlation coefficient (R)	0.68	0.84

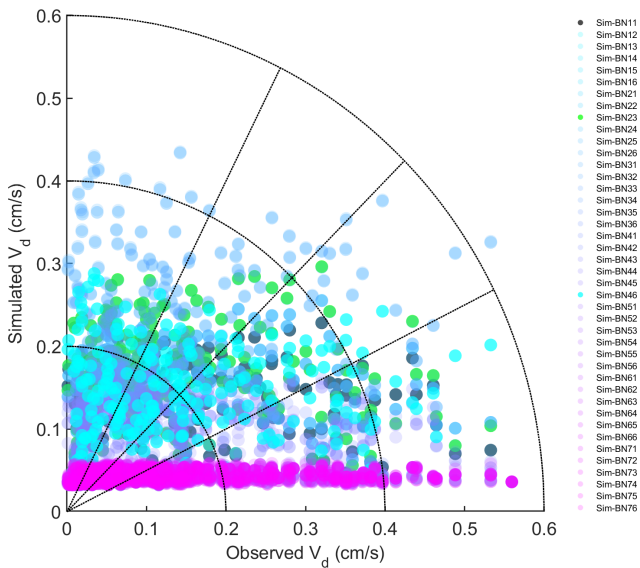


**Figure 2.** Comparison of observed and simulated  $V_d$  of  $\text{NO}_2$ .

Especially for the current version of the single-point Noah-MP-WDDM model, the concentration of  $\text{CO}_2$  is input to the model as a parameter, which may restrict the simulation performance of the model itself. When Noah-MP-WDDM is coupled to climate or atmospheric models, it may create new sources of uncertainty. The overall underestimation under MNM-5 may be because the default parameters of the leaf carbon–nitrogen ratio ( $C:N_{\text{leaf}}$ ) in the Biome-BGC model and single-point Noah-MP-WDDM model do not match the situation of subtropical forests.

However, we can still see the variation of the simulation bias caused by different mechanisms from the statistical results (Fig. 3). Most of the simulated combinations underestimate the average dry deposition velocity, but only three mechanism combinations – BN-16, BN-26 and BN-36 – overestimate it. It can be seen that the average simulation bias of BN-23 is the lowest among all mechanism combinations. Compared with the default BN-11 mechanism, its average bias is reduced from  $-0.0371$  to  $-0.0185 \text{ cm s}^{-1}$ , which reduces the relative deviation about 50.1 %. At the same time, BN-13 and BN-33 achieve similar results, with a simulation bias of the dry deposition velocity of  $-0.0187 \text{ cm s}^{-1}$ .

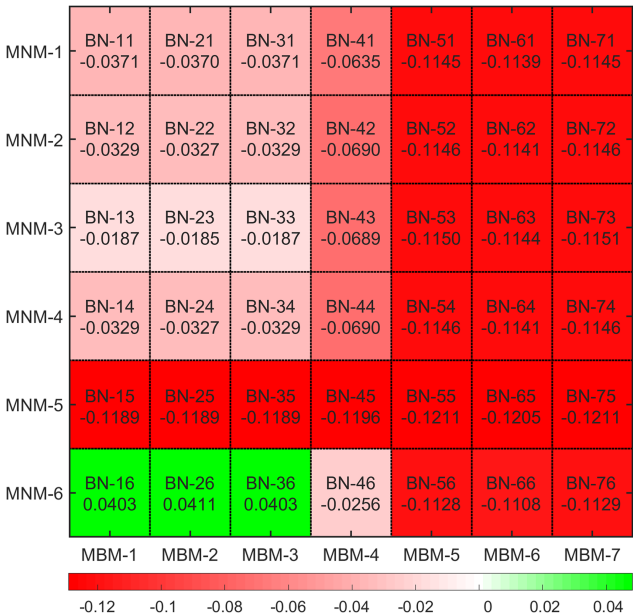


**Figure 3.** Mean bias of observed and simulated  $V_d$ .

Thus, for BN-46 the bias of dry deposition velocity is  $-0.0256 \text{ cm s}^{-1}$ .

**3.3 Implications for diurnal simulation of  $\text{NO}_2$  dry deposition velocity**

Although the ability of the models to simulate trends is statistically weak and the absolute difference in the average dry deposition velocity obtained from simultaneous results is small, we can still see that the model captures certain dry deposition characteristics from the daily cycle changes. Figure 4 uses a daily variation curve to show the simulation results of the effects of each mechanism combination on the dry deposition velocity. It can be seen that different mechanisms still show considerable pattern differences for the daily variation of  $\text{NO}_2$  dry deposition velocity.

The red line in Fig. 4 is the daily change in the observed value. Note the large fluctuation of its standard deviation, indicating a large fluctuation during the  $V_d$  observation period. This is because of the turbulent exchange caused by the fragmentation of the boundary layer inside and outside



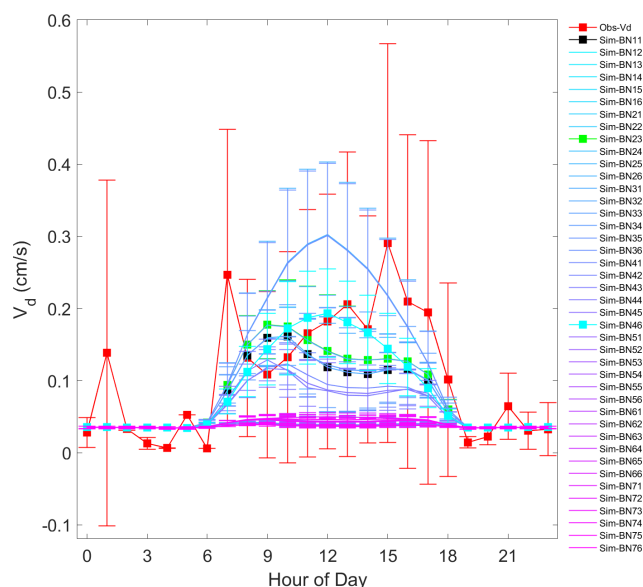


**Figure 4.** Diurnal variation of observed and simulated  $V_d$ .

the mountain forest canopy and the effect that the change in atmospheric stability has on the turbulence (Zhang et al., 2017). The black line in Fig. 4 corresponds to experiment BN-11, and the green line corresponds to BN-23. It can be seen that the simulated  $V_d$  values of BN-23 are increased mainly during the day compared to the original BN-11. At the same time, it can be seen that the standard deviation range of the observed values can basically cover the range of the simulated results. This could partly reflect the stability of the model, which may mean that these improved mechanisms can show similar performance when transplanted to other similar types of forests.

In addition, it is worth noting that some deposition observation studies believe that the  $V_d$  value at midday is the most noteworthy (Kavassalis and Murphy, 2017; Ke et al., 2020). Therefore, we also pay attention to the mechanism with the minimum bias at midday, which is BN-46. It can be seen that the simulated value of BN-46 is basically consistent with the  $V_d$  observation, with a bias of about  $0.001 \text{ cm s}^{-1}$  at midday.

Overall, the simulation of the daily variation of  $V_d$  presents four groups: the greatly underestimated group (represented by BN-55), the greatly overestimated group (represented by BN-26), the morning-higher and afternoon-lower pattern group (represented by BN-23), and the accurate-at-noon group (represented by BN-46). The original Noah-MP-WDDM (BN-11) belongs to the same group as BN-23 because their theoretical assumptions are consistent. The appearance of this grouping is quite interesting because it illustrates that there are relative differences in theoretical assumptions about stomatal resistance and nitrogen limits for photosynthesis. Therefore, in the next section we will discuss the effects of these improved scheme groups from the perspective of canopy deposition resistances with the four

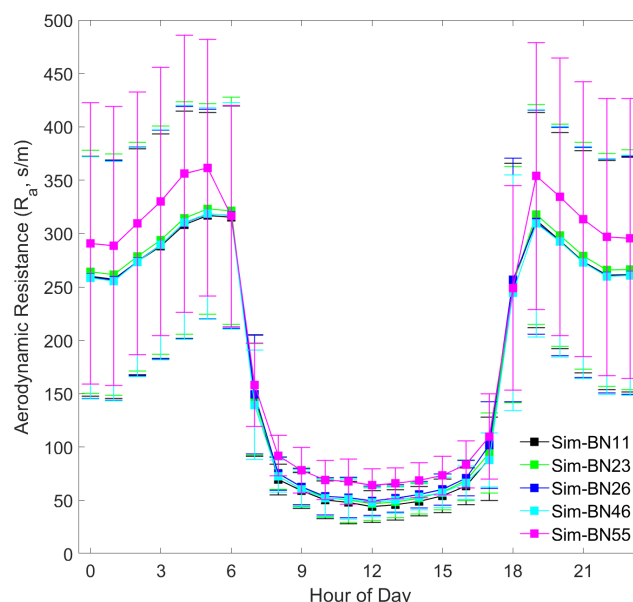


**Figure 5.** Diurnal variation of simulated  $R_a$ .

representative combinations and the Noah-MP-WDDM default combination (BN-11).

### 3.4 Comparison of modelled resistance components

#### 3.4.1 Aerodynamic and quasi-laminar boundary layer resistance

It can be seen that different mechanism improvements have relatively little impact on aerodynamic resistance ( $R_a$ ) and quasi-laminar boundary layer resistance ( $R_b$ ) since the improved mechanisms are concentrated in the canopy process. The four combinations of BN-11, BN-23, BN-26 and BN-46 are basically the same (BN-55 is the exception), as shown in Figs. 5 and 6. The differences in  $R_a$  between BN-55 and the other four combinations are present mainly during the night and are about  $30 \text{ s m}^{-1}$ , while the differences in  $R_b$  range between about 5 and  $10 \text{ s m}^{-1}$  during both the day and night.

However, the source of this difference for  $R_a$  and  $R_b$  is slightly different. The disturbance to  $R_a$  is indirectly caused by the calculation of Mourning–Obukhov length ( $L$ ) and friction velocity ( $u^*$ ) in the calculation of turbulence by the sensible and latent heat flux exchange controlled by the canopy stomatal mechanism. The disturbance of  $R_b$  is only indirectly affected by the calculation of  $u^*$ .

In addition, it is worth noting that the diurnal variation of  $R_b$  is more consistent with the observed  $V_d$ , which echoes the hypothesis of turbulence exchange caused by the breakage of the inner and outer boundary layers of the mountain forest canopy and changes in atmospheric stability proposed by Zhang et al. (2017). The model needs to express these situations by accurately expressing the forest structure.



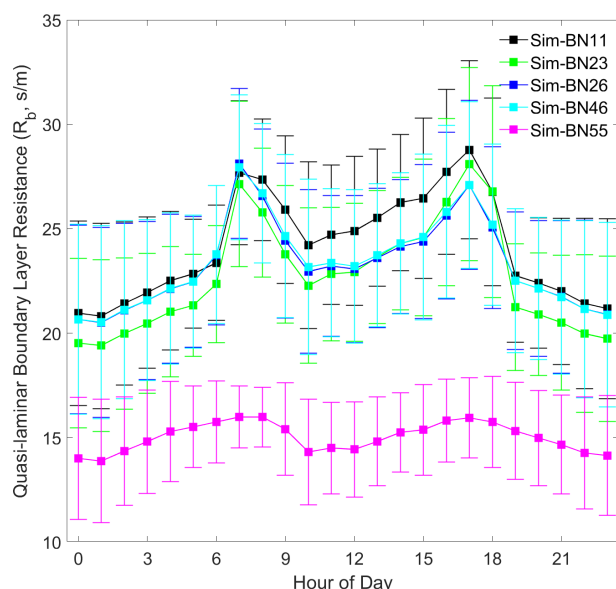


Figure 6. Diurnal variation of simulated  $R_b$ .

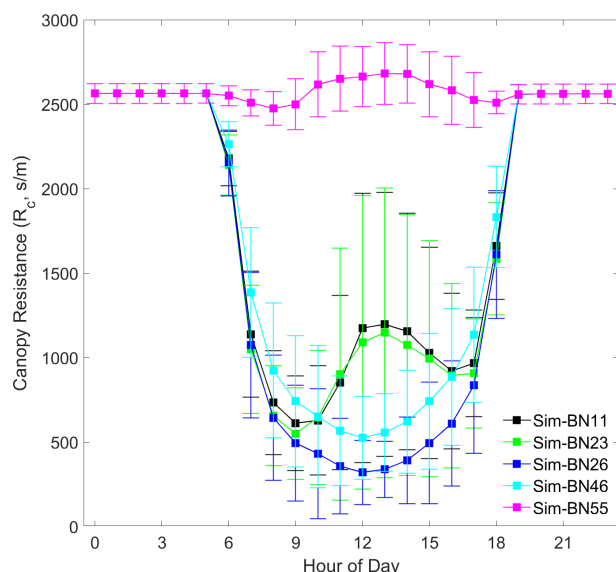


Figure 7. Diurnal variation of simulated  $R_c$ .

### 3.4.2 Canopy resistance

The difference in the simulation of the canopy resistance ( $R_c$ ) of each improvement scheme is the main source of the difference in the simulations of the dry deposition process, as shown in Fig. 7. It can be seen that for the consistently underestimated group represented by BN-55, the underestimation of deposition velocity comes from a large overestimation of  $R_c$ , indicating that the assumptions of these mechanisms are not suitable for subtropical forests as a whole. It is possible to draw inappropriate conclusions on such underlying surfaces from the source model results.

For BN-11 and BN-23, it can be seen that their theoretical hypotheses are the same, which can effectively reflect the physiological process of the increase in stomatal resistance caused by the closure of stomata at noon. The degree of stomatal reopening in the afternoon is slightly weaker, which makes the diurnal dry deposition velocity curve high in the morning and low in the afternoon. This is correct in a general sense, but there is a certain mismatch between the simulation and the observed results (low in the morning and high in the afternoon). We estimate that because the flux tower of the sample site of Dinghushan is located on a westward slope, the physiological activity of the vegetation canopy is weaker in the morning and stronger in the afternoon. This indicates that for model improvement, the parameterisation of the difference between sunlit and shaded leaves should be strengthened (otherwise it will be difficult to express this phenomenon).

It can be seen that the theoretical hypotheses for BN-26 and BN-46 are also the same but that neither can reflect the closure of stomata at noon. The difference is reflected mainly in the intensity of the decrease in  $R_c$  during the day, and the amplitude of the disturbance to the deposition velocity is greatly enhanced when the deposition resistance is lower than  $1000 \text{ s m}^{-1}$ . It can be seen from Figs. 4 and 7 that the difference in the deposition velocity curves obtained by the simulation of BN-26 and BN-46 is not yet apparent at 07:00 LT in the morning. At 12:00 LT, the difference in canopy resistance, which is only about  $200 \text{ s m}^{-1}$  lower, causes the BN-26 group to greatly overestimate deposition velocity. Under this series of mechanisms, the misestimation or disturbance of key parameters is likely to change the expected results.

## 4 Discussion

We improved upon the early Noah-MP-WDDM version, and our results emphasise that the importance of the canopy stomatal carbon dioxide compensation mechanism and the GPP-controlled leaf nitrogen-limiting factor for the simulation of nitrogen deposition are both overstated. All of the classic model mechanisms do a fairly poor job at capturing the deposition velocity of reactive nitrogen at the chosen site, which indicates that there are substantial gaps in our current understanding and parameterisation of in-canopy processes.

From a model point of view, some articles have begun to consider the internal processes of the canopy. For example, some models divide the process in the canopy into multiple layers, trying to distribute the radiation energy and the profile in the canopy more accurately, but it is only divided into non-stomatal and stomatal pathways for the material exchange process in the canopy, while the parameterisation of non-stomata is often set to various empirical constants (Bonan et al., 2021). There are some experiments that assume that the process of plant surface may not be as simple as we thought in the past, and thus different parameters are set for the wet

surface and the dry surface (Jia et al., 2016). However, the processes were just parameterisation using constants lacking physical meaning in different surface conditions. Recent isotope observational evidence also shows that forest canopies can retain nitrogen from atmospheric deposition and that the canopy N processing could alter the N supply and photosynthesis of the leaf in the short term (Wang et al., 2021a). For the simulation of non-stomatal processes on the surface of plants, more in-depth observations or open-top air chamber experiments are needed for support (Fisher and Koven, 2020).

At the same time, the stomatal pathway is in fact derived from empirical fitting in the field of atmospheric environmental research (Schwede et al., 2011), regardless as to whether it is using the Jarvis scheme or the Ball–Berry scheme. Although it has a classical photosynthesis mechanism for C3 and C4 plants separately, the parametric description of models basically does not consider the physiological response process and environmental adaptation process of the plant from the level of the plant's own gene control mechanism (Liang et al., 2020; Durand et al., 2021). In addition, the improvement of canopy structure measurement based on technologies such as lidar also requires corresponding parameterised simulation work to improve the characterisation of leaf morphological parameters in the canopy (Braghiere et al., 2021; Wang et al., 2021b). It is unrealistic to consider such in-depth consideration in the land surface model at this stage, but we believe that the consideration of biological physiological processes needs to be continuously refined while the understanding of the land–atmosphere exchange process in the ecosystem grows. For example, the biogeochemical processes, such as under-canopy diffusion process of reactive nitrogen oxides, the emission of volatile organic compounds from low-canopy vegetation under nitrogen stress, the photochemical reaction through the canopy gap, the emission of soil nitrogen components, and the coupling process of carbon and nitrogen ratio (Weathers et al., 2001; Finnigan et al., 2009; Flechard et al., 2013; Dentener et al., 2014; Erisman et al., 2014; Makar et al., 2017; Moon et al., 2019; Guerrieri et al., 2020; Ke et al., 2020; Wang et al., 2021a), all have effects on the exchange of nitrogen oxides at the interface inside the canopy and are worthy of parameterisation research.

We also compared the observed dry deposition velocity results carried out on different underlying surfaces and the simulated results using the different deposition resistance mechanisms coupled in this work, as shown in Table 4. It can be seen that the dry deposition velocities of the NO<sub>2</sub> range obtained by most of the model results is basically lower than the observed value obtained by the eddy correlation method, which is relatively consistent with the performance of most of the mechanism simulation results in this study. It can also be inferred from this that most of the regional models that adopt the default Wesely deposition mechanism, such as WRF-Chem, CMAQ and other widely used models,

may underestimate the dry nitrogen deposition flux (Chang et al., 2020a). The potential impact of this underestimation deserves in-depth discussion by the entire nitrogen deposition research community.

The sources of simulation uncertainty in this study may mainly come from the following aspects. The first aspect is the lack of observational data. Although the observational data used in this research have supported the publication of related articles in the previous period, the overall data quality is not good (Zhang et al., 2017; Chang et al., 2020b). The observational conditions in subtropical forests make it difficult to set up a long-term observation in nature reserves (Tian et al., 2018). Meanwhile, the observation needs to eliminate many interference factors in the measurement, and thus there are fewer data that meet the quality requirements in the end (Xu et al., 2015). Second, this study used Noah-MP's default lookup tables in terms of model input parameters. The parameters are not localised in this study. Quite a few parameters in them are empirical values, the average value of large-scale remote sensing or the average value of similar underlying surfaces (Niu et al., 2011; Dai et al., 2019; Massad et al., 2020). In this regard, we believe that it is necessary to further carry out the measurement and accurate characterisation of model parameters, especially vegetation canopy parameters and soil parameters, in order to further effectively reduce the uncertainty of the simulation, and to more clearly analyse the different effects of deposition resistance mechanisms.

## 5 Conclusions

In using Noah-MP-WDDM to study dry deposition processes, we implemented new features and applied several corrections to the code. Compared to Noah-MP-WDDM v1, the improvement of the canopy stomatal resistance mechanism and the nitrogen-limiting schemes in Noah-MP-WDDM v1.42 gives new options for simulating nitrogen dry deposition velocity. Our discussion shows that the major source of the difference in the simulations of the dry deposition process is the difference in the simulation of the  $R_c$  of each improvement scheme. The canopy stomatal and leaf nitrogen-limiting mechanisms from various classic models cannot express the diurnal changes in leaf canopy resistance well, especially the underestimation in the daytime, and present four sets of distributions via combination of the Yu et al. (2004) and Thornton et al. (2002) mechanisms (BN-55) and the effect of the Cao and Woodward (1998) mechanism on stomatal closure (MNM-6) at noon. This may be a source of bias in the simulation of nitrogen deposition flux by these mechanisms' source models.

Our results emphasise the importance of the canopy stomatal carbon dioxide compensation mechanism and the GPP-controlled leaf nitrogen-limiting factor for the simulation of nitrogen deposition. Considering the combination of these

**Table 4.** Comparison of NO<sub>2</sub> dry deposition velocities with some other studies.

Station	Land surface type	Method	$V_d$ (cm s <sup>-1</sup> )	Reference
Leende, NL	Grassland	Eddy correlation method	0.1–0.35	Coe and Gallagher (1992)
Elspeetsche, NL	Grassland	Gradient method	0.1–0.4	Erismann et al. (1994)
Harvard Forest, USA	Coniferous forests	Eddy correlation method	0.60–0.86	Wu et al. (2011, 2012)
California, USA	Laboratory measurements	Laser-induced fluorescence detection method	0.15–0.51	Delaria and Cohen (2020)
Hohenpeißenberg, DE	Coniferous forests	Eddy correlation method	0.01–0.45	Stella et al. (2013)
Birmingham, UK	Cropland	Inferential method (Wesely scheme)	0.16	Marnier and Harrison (2004)
EMEP monitors	Forest	Inferential method (Wesely scheme)	0.15	Flechard et al. (2011)
..	Grassland	Inferential method	0.12	..
..	Cropland	Inferential method	0.10	..
CAPMON monitors	Coniferous forests	Inferential method (Zhang scheme)	0.16–0.28	Zhang et al. (2009)
...	Broadleaf forests	Inferential method	0.13	...
...	Grassland	Inferential method	0.11–0.22	...
...	Cropland	Inferential method	0.07	...
Northern China	Forests	Inferential method (Wesely scheme)	0.02–0.09	Pan et al. (2012)
Central Africa	Forests	Inferential method (Wesely scheme)	0.31–0.33	Adon et al. (2013)

two mechanisms (BN-23 schemes in Noah-MP-WDDM v1.42 instead of Noah-MP-WDDM v1), it reduced the average simulation bias by about 50.1 %.

Our future work will focus on applying the combination of these mechanisms to the regional and global Noah-MP-WDDM model to simulate dry deposition for other surface types and other components. We hope to gain a deeper understanding of the simulation performance of canopy stomatal and leaf nitrogen-limiting mechanisms for dry deposition to learn more about the response and feedback of ecosystems and nitrogen deposition.

**Code and data availability.** The current version of model is available from the project website (<https://zenodo.org/record/4756246>, last access: 13 May 2021) under the Creative Commons Attribution 4.0 International license. The exact version of the model used to produce the results used in this paper is archived on Zenodo (<https://doi.org/10.5281/zenodo.4756246>, Chang, 2021a), and all the simulation results are presented on Zenodo (<https://doi.org/10.5281/zenodo.4756316>, Chang, 2021b).

**Author contributions.** MC designed the research, conducted the model development and drafted the paper. JC performed the model simulation and drafted the paper. QZ and WC did the Noah-MP-WDDM code review. GW and LW did the model output analysis. WW polished the work. MC was supervised directly by XW during the model development work. All authors contributed to the interpretation of the results.

**Competing interests.** The contact author has declared that neither they nor their co-authors have any competing interests.

**Disclaimer.** Publisher's note: Copernicus Publications remains neutral with regard to jurisdictional claims in published maps and institutional affiliations.

**Acknowledgements.** Calculations for this work were supported by The High Performance Public Computing Service Platform of Jinan University. We thank Laurel Anderton for her linguistic assistance during the preparation of this paper.

**Financial support.** This research has been supported by the National Key Research and Development Program of China (grant no. 2017YFC0210103), the National Natural Science Foundation of China (grant nos. 41705123 and 41905086), the Special Fund Project for Science and Technology Innovation Strategy of Guangdong Province (grant no. 2019B121205004), and the Guangdong Innovative and Entrepreneurial Research Team Program (grant no. 2016ZT06N263).

**Review statement.** This paper was edited by Jatin Kala and reviewed by two anonymous referees.

## References

- Aber, J. D. and Federer, C. A.: A generalized, lumped-parameter model of photosynthesis, evapotranspiration and net primary production in temperate and boreal forest ecosystems, *Oecologia*, 92, 463–474, 1992.
- Adon, M., Galy-Lacaux, C., Delon, C., Yoboue, V., Solmon, F., and Kaptue Tchente, A. T.: Dry deposition of nitrogen compounds ( $\text{NO}_2$ ,  $\text{HNO}_3$ ,  $\text{NH}_3$ ), sulfur dioxide and ozone in west and central African ecosystems using the inferential method, *Atmos. Chem. Phys.*, 13, 11351–11374, <https://doi.org/10.5194/acp-13-11351-2013>, 2013.
- Aphalo, P. and Jarvis, P.: An analysis of Ball's empirical model of stomatal conductance, *Ann. Bot.*, 72, 321–327, 1993.
- Ball, J. T., Woodrow, I. E., and Berry, J. A.: A model predicting stomatal conductance and its contribution to the control of photosynthesis under different environmental conditions, in: *Progress in photosynthesis research*, edited by: Biggins, J., Springer, Dordrecht, 221–224, [https://doi.org/10.1007/978-94-017-0519-6\\_48](https://doi.org/10.1007/978-94-017-0519-6_48), 1987.
- Bernhard, A.: The nitrogen cycle: Processes, players, and human impact, *Nature Education Knowledge*, 3, 25, 2012.
- Bonan, G. B.: Land-atmosphere  $\text{CO}_2$  exchange simulated by a land surface process model coupled to an atmospheric general, *J. Geophys. Res.*, 100, 2817–2831, 1995.
- Bonan, G. B., Patton, E. G., Finnigan, J. J., Baldocchi, D. D., and Harman, I. N.: Moving beyond the incorrect but useful paradigm: reevaluating big-leaf and multilayer plant canopies to model biosphere-atmosphere fluxes – a review, *Agr. Forest Meteorol.*, 306, 108435, 2021.
- Braghiere, R. K., Wang, Y., Doughty, R., Sousa, D., Magney, T., Widlowski, J.-L., Longo, M., Bloom, A. A., Worden, J., Gentile, P., and Frankenberg, C.: Accounting for canopy structure improves hyperspectral radiative transfer and sun-induced chlorophyll fluorescence representations in a new generation Earth System model, *Remote Sens. Environ.*, 261, 112497, <https://doi.org/10.1016/j.rse.2021.112497>, 2021.
- Cao, M. and Woodward, F. I.: Net primary and ecosystem production and carbon stocks of terrestrial ecosystems and their responses to climate change, *Glob. Change Biol.*, 4, 185–198, 1998.
- Chang, M.: Noah-MP-WDDMv1.42 code, Version 1.42, Zenodo [code], <https://doi.org/10.5281/zenodo.4756246>, 2021a (code available at: <https://zenodo.org/record/4756246>, last access: 13 May 2021).
- Chang, M.: The result data of Noah-MP-WDDMv1.42, Version 1, Zenodo [data set], <https://doi.org/10.5281/zenodo.4756316>, 2021b.
- Chang, M., Cao, J., Ma, M., Liu, Y., Liu, Y., Chen, W., Fan, Q., Liao, W., Jia, S., and Wang, X.: Dry deposition of reactive nitrogen to different ecosystems across eastern China: A comparison of three community models, *Sci. Total Environ.*, 720, 137548, <https://doi.org/10.1016/j.scitotenv.2020.137548>, 2020a.
- Chang, M., Liao, W., Wang, X., Zhang, Q., Chen, W., Wu, Z., and Hu, Z.: An optimal ensemble of the Noah-MP land surface model for simulating surface heat fluxes over a typical subtropical forest in South China, *Agr. Forest Meteorol.*, 281, 107815, 2020b.
- Chen, W., Chen, J., and Cihlar, J.: An integrated terrestrial ecosystem carbon-budget model based on changes in disturbance, climate, and atmospheric chemistry, *Ecol. Model.*, 135, 55–79, 2000.
- Coe, H. and Gallagher, M.: Measurements of Dry Deposition of  $\text{NO}_2$  to A Dutch Heathland Using the Eddy-Correlation Technique, *Q. J. Roy. Meteor. Soc.*, 118, 767–786, 1992.
- Cui, J., Zhou, J., and Yang, H.: Atmospheric inorganic nitrogen in dry deposition to a typical red soil agro-ecosystem in southeastern China, *J. Environ. Monitor.*, 12, 1287–1294, 2010.
- Dai, Y., Dickinson, R. E., and Wang, Y.-P.: A two-big-leaf model for canopy temperature, photosynthesis, and stomatal conductance, *J. Climate*, 17, 2281–2299, 2004.
- Dai, Y., Yuan, H., Xin, Q., Wang, D., Shangguan, W., Zhang, S., Liu, S., and Wei, N.: Different representations of canopy structure – A large source of uncertainty in global land surface modeling, *Agr. Forest Meteorol.*, 269, 119–135, 2019.
- De Kauwe, M. G., Kala, J., Lin, Y.-S., Pitman, A. J., Medlyn, B. E., Duursma, R. A., Abramowitz, G., Wang, Y.-P., and Miralles, D. G.: A test of an optimal stomatal conductance scheme within the CABLE land surface model, *Geosci. Model Dev.*, 8, 431–452, <https://doi.org/10.5194/gmd-8-431-2015>, 2015.
- De Vries, W., Posch, M., Reinds, G. J., and Hettelingh, J.-P.: Quantifying relationships between N deposition and impacts on forest ecosystem services, Progress in the modelling of critical thresholds, impacts to plant species diversity and ecosystem services in Europe, Coordination Centre for Effects, Bilthoven, The Netherlands, Status Report, 43–53, 2009.
- Delaria, E. R. and Cohen, R. C.: A model-based analysis of foliar  $\text{NO}_x$  deposition, *Atmos. Chem. Phys.*, 20, 2123–2141, <https://doi.org/10.5194/acp-20-2123-2020>, 2020.
- Delaria, E. R., Vieira, M., Cremieux, J., and Cohen, R. C.: Measurements of  $\text{NO}$  and  $\text{NO}_2$  exchange between the atmosphere and *Quercus agrifolia*, *Atmos. Chem. Phys.*, 18, 14161–14173, <https://doi.org/10.5194/acp-18-14161-2018>, 2018.
- Dentener, F., Vet, R., Dennis, R. L., Du, E., Kulshrestha, U. C., and Galy-Lacaux, C.: Progress in Monitoring and Modelling Estimates of Nitrogen Deposition at Local, Regional and Global Scales, in: *Nitrogen Deposition, Critical Loads and Biodiversity*, Springer, 7–22, [https://doi.org/10.1007/978-94-007-7939-6\\_2](https://doi.org/10.1007/978-94-007-7939-6_2), 2014.
- Durand, M., Murchie, E. H., Lindfors, A. V., Urban, O., Aphalo, P. J., and Robson, T. M.: Diffuse solar radiation and canopy photosynthesis in a changing environment, *Agr. Forest Meteorol.*, 311, 108684, <https://doi.org/10.1016/j.agrformet.2021.108684>, 2021.
- Erisman, J., van Elzakker, B., Mennen, M., Hogenkamp, J., Zwart, E., van den Beld, L., Römer, F., Bobbink, R., Heil, G., Raessen, M., Duyzer, J. H., Verhage, H., Wyers, G. P., Otjes, R. P., and Möls, J. J.: The Elspeetsche Veld experiment on surface exchange of trace gases: summary of results, *Atmos. Environ.*, 28, 487–496, 1994.
- Erisman, J. W., Leach, A., Adams, M., Agboola, J. I., Ahmetaj, L., Alard, D., Austin, A., Awodun, M. A., Bareham, S., Bird, T. L., Bleeker, A., Bull, K., Cornell, S. E., Davidson, E., de Vries, W., Dias, T., Emmett, B., Goodale, C., Greaver, T., Haeuber, R., Harmens, H., Hicks, W. K., Hogbom, L., Jarvis, P., Johansson, M., Russell, Z., McClean, C., Paton, B., Perez, T., Plesnik, J., Rao, N., Schmidt, S., Sharma, Y. B., Tokuchi, N., and Whitfield, C. P.: Nitrogen deposition effects on ecosystem services and interactions with other pollutants and climate change, in: *Nitrogen*

- deposition, critical loads and biodiversity, edited by: Sutton, M., Mason, K., Sheppard, L., Sverdrup, H., Haeuber, R., and Hicks, W., Springer, Dordrecht, 493–505, [https://doi.org/10.1007/978-94-007-7939-6\\_51](https://doi.org/10.1007/978-94-007-7939-6_51), 2014.
- Falge, E., Reth, S., Brüggemann, N., Butterbach-Bahl, K., Goldberg, V., Oltchev, A., Schaaf, S., Spindler, G., Stiller, B., Queck, R., Köstner, B., and Bernhofer, C.: Comparison of surface energy exchange models with eddy flux data in forest and grassland ecosystems of Germany, *Ecol. Model.*, 188, 174–216, 2005.
- Farquhar, G., von Caemmerer, S., and Berry, J.: A biochemical model of photosynthetic CO<sub>2</sub> assimilation in leaves of C3 species, *Planta*, 149, 78–90, 1980.
- Finnigan, J.: Turbulence in plant canopies, *Annu. Rev. Fluid Mech.*, 32, 519–571, 2000.
- Finnigan, J. J., Shaw, R. H., and Patton, E. G.: Turbulence structure above a vegetation canopy, *J. Fluid Mech.*, 637, 387–424, 2009.
- Fisher, R. A. and Koven, C. D.: Perspectives on the future of land surface models and the challenges of representing complex terrestrial systems, *J. Adv. Model. Earth Sy.*, 12, e2018MS001453, <https://doi.org/10.1029/2018MS001453>, 2020.
- Flechard, C. R., Nemitz, E., Smith, R. I., Fowler, D., Vermeulen, A. T., Bleeker, A., Erisman, J. W., Simpson, D., Zhang, L., Tang, Y. S., and Sutton, M. A.: Dry deposition of reactive nitrogen to European ecosystems: a comparison of inferential models across the NitroEurope network, *Atmos. Chem. Phys.*, 11, 2703–2728, <https://doi.org/10.5194/acp-11-2703-2011>, 2011.
- Flechard, C. R., Massad, R.-S., Loubet, B., Personne, E., Simpson, D., Bash, J. O., Cooter, E. J., Nemitz, E., and Sutton, M. A.: Advances in understanding, models and parameterizations of biosphere-atmosphere ammonia exchange, *Biogeosciences*, 10, 5183–5225, <https://doi.org/10.5194/bg-10-5183-2013>, 2013.
- Friedlingstein, P., Joel, G., Field, C. B., and Fung, I. Y.: Toward an allocation scheme for global terrestrial carbon models, *Glob. Change Biol.*, 5, 755–770, 1999.
- Galloway, J. N., Hiram Levy, I., and Kasibhatla, P. S.: Year 2020: Consequences of population growth and development on deposition of oxidized nitrogen, *Ambio*, 23, 120–123, 1994.
- Ganzeveld, L., Lelieveld, J., Dentener, F., Krol, M., and Roelofs, G.-J.: Atmosphere-biosphere trace gas exchanges simulated with a single-column model, *J. Geophys. Res.*, 107, ACH 8-1–ACH 8-21, 2002.
- Gruber, N. and Galloway, J. N.: An Earth-system perspective of the global nitrogen cycle, *Nature*, 451, 293–296, 2008.
- Guerrieri, R., Lecha, L., Mattana, S., Cáliz, J., Casamayor, E. O., Barceló, A., Michalski, G., Peñuelas, J., Avila, A., and Mencuccini, M.: Partitioning between atmospheric deposition and canopy microbial nitrification into throughfall nitrate fluxes in a Mediterranean forest, *J. Ecol.*, 108, 626–640, 2020.
- Han, X., Zhang, M., Skorokhod, A., and Kou, X.: Modeling dry deposition of reactive nitrogen in China with RAMS-CMAQ, *Atmos. Environ.*, 166, 47–61, 2017.
- Horii, C. V., Munger, J. W., Wofsy, S. C., Zahniser, M., Nelson, D., and McManus, J. B.: Atmospheric reactive nitrogen concentration and flux budgets at a Northeastern US forest site, *Agr. Forest Meteorol.*, 133, 210–225, 2005.
- Jarvis, P.: The interpretation of the variations in leaf water potential and stomatal conductance found in canopies in the field, *Philos. T. Roy. Soc. B*, 273, 593–610, 1976.
- Jefferies, R. L. and Maron, J. L.: The embarrassment of riches: atmospheric deposition of nitrogen and community and ecosystem processes, *Trends. Ecol. Evol.*, 12, 74–78, 1997.
- Ji, J.: A climate-vegetation interaction model: Simulating physical and biological processes at the surface, *J. Biogeogr.*, 22, 445–451, 1995.
- Jia, Y., Yu, G., Gao, Y., He, N., Wang, Q., Jiao, C., and Zuo, Y.: Global inorganic nitrogen dry deposition inferred from ground-and space-based measurements, *Sci. Rep.*, 6, 19810, <https://doi.org/10.1038/srep19810>, 2016.
- Katul, G. G., Oren, R., Manzoni, S., Higgins, C., and Parlange, M. B.: Evapotranspiration: a process driving mass transport and energy exchange in the soil-plant-atmosphere-climate system, *Rev. Geophys.*, 50, RG3002, <https://doi.org/10.1029/2011RG000366>, 2012.
- Kavassalis, S. C. and Murphy, J. G.: Understanding ozone-meteorology correlations: A role for dry deposition, *Geophys. Res. Lett.*, 44, 2922–2931, <https://doi.org/10.1002/2016GL071791>, 2017.
- Ke, P., Yu, Q., Luo, Y., Kang, R., and Duan, L.: Fluxes of nitrogen oxides above a subtropical forest canopy in China, *Sci. Total Environ.*, 715, 136993, <https://doi.org/10.1016/j.scitotenv.2020.136993>, 2020.
- Landsberg, J. and Waring, R.: A generalised model of forest productivity using simplified concepts of radiation-use efficiency, carbon balance and partitioning, *Forest Ecol. Manag.*, 95, 209–228, 1997.
- Leuning, R.: Modelling stomatal behaviour and photosynthesis of *Eucalyptus grandis*, *Funct. Plant Biol.*, 17, 159–175, 1990.
- Leuning, R.: A critical appraisal of a combined stomatal-photosynthesis model for C3 plants, *Plant Cell Environ.*, 18, 339–355, 1995.
- Li, L., Huang, M., Gu, F., and Zhang, L.: The Modeling Algorithms for the Effects of Nitrogen on Terrestrial Vegetation Carbon Cycle Process, *Journal of Natural Resources*, 28, 2012–2022, 2013.
- Li, Y., Schichtel, B. A., Walker, J. T., Schwede, D. B., Chen, X., Lehmann, C. M., Puchalski, M. A., Gay, D. A., and Collett, J. L.: Increasing importance of deposition of reduced nitrogen in the United States, *P. Natl. Acad. Sci. USA*, 113, 5874–5879, 2016.
- Liang, X., Zhang, T., Lu, X., Ellsworth, D. S., BassiriRad, H., You, C., Wang, D., He, P., Deng, Q., Liu, H., Mo, J., and Ye, Q.: Global response patterns of plant photosynthesis to nitrogen addition: A meta-analysis, *Glob. Change Biol.*, 26, 3585–3600, 2020.
- Lin, B.-L., Sakoda, A., Shibasaki, R., Goto, N., and Suzuki, M.: Modelling a global biogeochemical nitrogen cycle in terrestrial ecosystems, *Ecol. Model.*, 135, 89–110, 2000.
- Liu, J., Chen, J., Cihlar, J., and Chen, W.: Net primary productivity distribution in the BOREAS region from a process model using satellite and surface data, *J. Geophys. Res.-Atmos.*, 104, 27735–27754, 1999.
- Liu, J., Price, D. T., and Chen, J. M.: Nitrogen controls on ecosystem carbon sequestration: a model implementation and application to Saskatchewan, Canada, *Ecol. Model.*, 186, 178–195, 2005.
- Liu, L., Zhang, X., Xu, W., Liu, X., Lu, X., Wei, J., Li, Y., Yang, Y., Wang, Z., and Wong, A. Y. H.: Reviewing global estimates of surface reactive nitrogen concentration and deposition using satellite retrievals, *Atmos. Chem. Phys.*, 20, 8641–8658, <https://doi.org/10.5194/acp-20-8641-2020>, 2020.

- Liu, X., Zhang, Y., Han, W., Tang, A., Shen, J., Cui, Z., Vitousek, P., Erisman, J. W., Goulding, K., Christie, P., Fangmeier, A., and Zhang, F.: Enhanced nitrogen deposition over China, *Nature*, 494, 459–462, 2013.
- Lohammar, T., Larsson, S., Linder, S., and Falk, S.: FAST: simulation models of gaseous exchange in Scots pine, *Ecol. Bull.*, 32, 505–523, 1980.
- Makar, P., Staebler, R., Akingunola, A., Zhang, J., McLinden, C., Kharol, S., Pabla, B., Cheung, P., and Zheng, Q.: The effects of forest canopy shading and turbulence on boundary layer ozone, *Nat. Commun.*, 8, 1–14, 2017.
- Marnier, B. and Harrison, R. M.: A spatially refined monitoring based study of atmospheric nitrogen deposition, *Atmos. Environ.*, 38, 5045–5056, 2004.
- Massad, R. S., Tuzet, A., Personne, E., Bedos, C., Beekmann, M., Coll, I., Drouet, J.-L., Fortems-Cheiney, A., Générmont, S., Loubet, B., and Saint-Jean, S.: Modelling Exchanges: From the Process Scale to the Regional Scale, in: *Agriculture and Air Quality*, Springer, 159–207, [https://doi.org/10.1007/978-94-024-2058-6\\_7](https://doi.org/10.1007/978-94-024-2058-6_7), 2020.
- McGuire, A. D., Melillo, J. M., Kicklighter, D. W., Pan, Y., Xiao, X., Helfrich, J., Moore, B., Vorosmarty, C. J., and Schloss, A. L.: Equilibrium responses of global net primary production and carbon storage to doubled atmospheric carbon dioxide: Sensitivity to changes in vegetation nitrogen concentration, *Global Biogeochem. Cy.*, 11, 173–189, 1997.
- Medlyn, B. E., Duursma, R. A., Eamus, D., Ellsworth, D. S., Prentice, I. C., Barton, C. V., Crous, K. Y., de Angelis, P., Freeman, M., and Wingate, L.: Reconciling the optimal and empirical approaches to modelling stomatal conductance, *Glob. Change Biol.*, 17, 2134–2144, 2011.
- Monteith, J.: Solar radiation and productivity in tropical ecosystems, *J. Appl. Ecol.*, 9, 747–766, 1972.
- Monteith, J. L. and Moss, C.: Climate and the efficiency of crop production in Britain [and discussion], *Philos. T. Roy. Soc. B*, 281, 277–294, 1977.
- Moon, K., Duff, T., and Tolhurst, K.: Sub-canopy forest winds: understanding wind profiles for fire behaviour simulation, *Fire Safety J.*, 105, 320–329, 2019.
- Niu, G.-Y.: The community NOAA land-surface model (LSM) with multi-physics options, User Guide, Center for Integrated Earth System Science, The University of Texas at Austin, Austin, TX, USA, Heritage, 1–21, 2011.
- Niu, G.-Y., Yang, Z.-L., Mitchell, K. E., Chen, F., Ek, M. B., Barlage, M., Kumar, A., Manning, K., Niyogi, D., Rosero, E., Tewari, M., and Xia, Y.: The community Noah land surface model with multiparameterization options (Noah-MP): 1. Model description and evaluation with local-scale measurements, *J. Geophys. Res.*, 116, D12109, <https://doi.org/10.1029/2010JD015139>, 2011.
- Niyogi, D., Alapaty, K., Raman, S., and Chen, F.: Development and evaluation of a coupled photosynthesis-based gas exchange evapotranspiration model (GEM) for mesoscale weather forecasting applications, *J. Appl. Meteorol. Clim.*, 48, 349–368, 2009.
- Oleson, K. W., Lawrence, D. M., Gordon, B., Flanner, M. G., Kluzek, E., Peter, J., Levis, S., Swenson, S. C., Thornton, E., Feddes, J., Heald, C. L., Hoffman, F., Lamarque, J.-F., Mahowald, N., Niu, G.-Y., Qian, T., Randerson, J., Running, S., Sakaguchi, K., Slater, A., Stockli, R., Wang, A., Yang, Z.-L., Zeng, X., and Zeng, X.: Technical description of version 4.0 of the Community Land Model (CLM), University Corporation for Atmospheric Research, 2010.
- Pan, Y. P., Wang, Y. S., Tang, G. Q., and Wu, D.: Wet and dry deposition of atmospheric nitrogen at ten sites in Northern China, *Atmos. Chem. Phys.*, 12, 6515–6535, <https://doi.org/10.5194/acp-12-6515-2012>, 2012.
- Peng, C., Liu, J., Dang, Q., Apps, M. J., and Jiang, H.: TRIPLEX: a generic hybrid model for predicting forest growth and carbon and nitrogen dynamics, *Ecol. Model.*, 153, 109–130, 2002.
- Phillips, S. B., Aneja, V. P., Kang, D., and Arya, S. P.: Modelling and analysis of the atmospheric nitrogen deposition in North Carolina, *International Journal of Global Environmental Issues*, 6, 231–252, 2006.
- Place, B. K., Delaria, E. R., Liu, A. X., and Cohen, R. C.: Leaf Stomatal Control over Acyl Peroxynitrate Dry Deposition to Trees, *ACS Earth and Space Chemistry*, 4, 2162–2170, 2020.
- Schulz, M., Prospero, J. M., Baker, A. R., Dentener, F., Ickes, L., Liss, P. S., Mahowald, N. M., Nickovic, S., García-Pando, C. P., Rodríguez, S., Sarin, M., Tegen, I., and Duce, R. A.: Atmospheric transport and deposition of mineral dust to the ocean: implications for research needs, *Environ. Sci. Technol.*, 46, 10390–10404, 2012.
- Schwede, D., Zhang, L., Vet, R., and Lear, G.: An intercomparison of the deposition models used in the CASTNET and CAPMoN networks, *Atmos. Environ.*, 45, 1337–1346, 2011.
- Seinfeld, J. H. and Pandis, S. N.: *Atmospheric chemistry and physics: from air pollution to climate change*, John Wiley & Sons, ISBN: 978-1-118-94740-1, 2012.
- Simpson, D., Benedictow, A., Berge, H., Bergström, R., Emberson, L. D., Fagerli, H., Flechard, C. R., Hayman, G. D., Gauss, M., Jonson, J. E., Jenkin, M. E., Nyíri, A., Richter, C., Semeena, V. S., Tsyro, S., Tuovinen, J.-P., Valdebenito, Á., and Wind, P.: The EMEP MSC-W chemical transport model – technical description, *Atmos. Chem. Phys.*, 12, 7825–7865, <https://doi.org/10.5194/acp-12-7825-2012>, 2012.
- Stella, P., Kortner, M., Ammann, C., Foken, T., Meixner, F. X., and Trebs, I.: Measurements of nitrogen oxides and ozone fluxes by eddy covariance at a meadow: evidence for an internal leaf resistance to NO<sub>2</sub>, *Biogeosciences*, 10, 5997–6017, <https://doi.org/10.5194/bg-10-5997-2013>, 2013.
- Stevens, C. J., Dise, N. B., Mountford, J. O., and Gowing, D. J.: Impact of nitrogen deposition on the species richness of grasslands, *Science*, 303, 1876–1879, 2004.
- Szinyei, D.: Modelling and evaluation of ozone dry deposition, PhD thesis, Freie Universität Berlin, 2015.
- Thornton, P., Law, B., Gholz, H. L., Clark, K. L., Falge, E., Ellsworth, D., Goldstein, A., Monson, R., Hollinger, D., Falk, M., Chen, J., and Sparks, J. P.: Modeling and measuring the effects of disturbance history and climate on carbon and water budgets in evergreen needleleaf forests, *Agr. Forest Meteorol.*, 113, 185–222, 2002.
- Tian, D., Du, E., Jiang, L., Ma, S., Zeng, W., Zou, A., Feng, C., Xu, L., Xing, A., Wang, W., Zheng, C., Ji, C., Shen, H., and Fang, J.: Responses of forest ecosystems to increasing N deposition in China: A critical review, *Environ. Pollut.*, 243, 75–86, <https://doi.org/10.1016/j.envpol.2018.08.010>, 2018.
- Tian, H., Liu, M., Zhang, C., Ren, W., Xu, X., Chen, G., Lv, C., and Tao, B.: The Dynamic Land Ecosystem Model (DLEM) for



- simulating terrestrial processes and interactions in the context of multifactor global change, *Acta Geographica Sinica*, 65, 1027–1047, 2010.
- Wang, W., Ganzeveld, L., Rossabi, S., Hueber, J., and Helmig, D.: Measurement report: Leaf-scale gas exchange of atmospheric reactive trace species ( $\text{NO}_2$ ,  $\text{NO}$ ,  $\text{O}_3$ ) at a northern hardwood forest in Michigan, *Atmos. Chem. Phys.*, 20, 11287–11304, <https://doi.org/10.5194/acp-20-11287-2020>, 2020.
- Wang, X., Wang, B., Wang, C., Wang, Z., Li, J., Jia, Z., Yang, S., Li, P., Wu, Y., Pan, S., and Liu, L.: Canopy processing of N deposition increases short-term leaf N uptake and photosynthesis, but not long-term N retention for aspen seedlings, *New Phytol.*, 229, 2601–2610, 2021a.
- Wang, Y., Köhler, P., He, L., Doughty, R., Braghiere, R. K., Wood, J. D., and Frankenberg, C.: Testing stomatal models at the stand level in deciduous angiosperm and evergreen gymnosperm forests using CliMA Land (v0.1), *Geosci. Model Dev.*, 14, 6741–6763, <https://doi.org/10.5194/gmd-14-6741-2021>, 2021b.
- Weathers, K. C., Cadenasso, M. L., and Pickett, S. T.: Forest edges as nutrient and pollutant concentrators: potential synergisms between fragmentation, forest canopies, and the atmosphere, *Conserv. Biol.*, 15, 1506–1514, 2001.
- Wesely, M.: Parameterization of surface resistances to gaseous dry deposition in regional-scale numerical models, *Atmos. Environ.*, 23, 1293–1304, 1989.
- Wolfe, G. M. and Thornton, J. A.: The Chemistry of Atmosphere-Forest Exchange (CAFE) Model – Part 1: Model description and characterization, *Atmos. Chem. Phys.*, 11, 77–101, <https://doi.org/10.5194/acp-11-77-2011>, 2011.
- Woodward, F. I., Smith, T. M., and Emanuel, W. R.: A global land primary productivity and phytogeography model, *Global Biogeochem. Cy.*, 9, 471–490, 1995.
- Wu, Z., Wang, X., Chen, F., Turnipseed, A. A., Guenther, A. B., Niyogi, D., Charusombat, U., Xia, B., Munger, J. W., and Alapaty, K.: Evaluating the calculated dry deposition velocities of reactive nitrogen oxides and ozone from two community models over a temperate deciduous forest, *Atmos. Environ.*, 45, 2663–2674, 2011.
- Wu, Z., Wang, X., Turnipseed, A. A., Chen, F., Zhang, L., Guenther, A. B., Karl, T., Huey, L., Niyogi, D., Xia, B., and Alapaty, K.: Evaluation and improvements of two community models in simulating dry deposition velocities for peroxyacetyl nitrate (PAN) over a coniferous forest, *J. Geophys. Res.*, 117, D04310, <https://doi.org/10.1029/2011JD016751>, 2012.
- Wu, Z., Schwede, D. B., Vet, R., Walker, J. T., Shaw, M., Staebler, R., and Zhang, L.: Evaluation and Intercomparison of Five North American Dry Deposition Algorithms at a Mixed Forest Site, *J. Adv. Model. Earth Sy.*, 10, 1571–1586, <https://doi.org/10.1029/2017MS001231>, 2018.
- Xu, G.-L., Schleppi, P., Li, M.-H., and Fu, S.-L.: Negative responses of Collembola in a forest soil (Alptal, Switzerland) under experimentally increased N deposition, *Environ. Pollut.*, 157, 2030–2036, 2009.
- Xu, W., Luo, X. S., Pan, Y. P., Zhang, L., Tang, A. H., Shen, J. L., Zhang, Y., Li, K. H., Wu, Q. H., Yang, D. W., Zhang, Y. Y., Xue, J., Li, W. Q., Li, Q. Q., Tang, L., Lu, S. H., Liang, T., Tong, Y. A., Liu, P., Zhang, Q., Xiong, Z. Q., Shi, X. J., Wu, L. H., Shi, W. Q., Tian, K., Zhong, X. H., Shi, K., Tang, Q. Y., Zhang, L. J., Huang, J. L., He, C. E., Kuang, F. H., Zhu, B., Liu, H., Jin, X., Xin, Y. J., Shi, X. K., Du, E. Z., Dore, A. J., Tang, S., Collett Jr., J. L., Goulding, K., Sun, Y. X., Ren, J., Zhang, F. S., and Liu, X. J.: Quantifying atmospheric nitrogen deposition through a nationwide monitoring network across China, *Atmos. Chem. Phys.*, 15, 12345–12360, <https://doi.org/10.5194/acp-15-12345-2015>, 2015.
- Yang, R. and Friedl, M. A.: Modeling the effects of three-dimensional vegetation structure on surface radiation and energy balance in boreal forests, *J. Geophys. Res.*, 108, 8615, <https://doi.org/10.1029/2002JD003109>, 2003.
- Yang, Z.-L., Niu, G.-Y., Mitchell, K. E., Chen, F., Ek, M. B., Barlage, M., Longuevergne, L., Manning, K., Niyogi, D., Tewari, M., and Xia, Y.: The community Noah land surface model with multiparameterization options (Noah-MP): 2. Evaluation over global river basins, *J. Geophys. Res.*, 116, D12110, <https://doi.org/10.1029/2010JD015140>, 2011.
- Ye, Z.-P. and Yu, Q.: Comparison of new and several classical models of photosynthesis in response to irradiance, *Chinese Journal of Plant Ecology*, 32, 1356, 2008.
- Yongjiu, D. and Qingcun, Z.: A land surface model (IAP94) for climate studies part I: Formulation and validation in off-line experiments, *Adv. Atmos. Sci.*, 14, 433–460, 1997.
- Yu, G., Jia, Y., He, N., Zhu, J., Chen, Z., Wang, Q., Piao, S., Liu, X., He, H., Guo, X., Wen, Z., Li, P., Ding, G., and Goulding, K.: Stabilization of atmospheric nitrogen deposition in China over the past decade, *Nat. Geosci.*, 12, 424–429, 2019.
- Yu, Q., Zhang, Y., Liu, Y., and Shi, P.: Simulation of the stomatal conductance of winter wheat in response to light, temperature and  $\text{CO}_2$  changes, *Ann. Bot.*, 93, 435–441, 2004.
- Zhang, L., Brook, J. R., and Vet, R.: A revised parameterization for gaseous dry deposition in air-quality models, *Atmos. Chem. Phys.*, 3, 2067–2082, <https://doi.org/10.5194/acp-3-2067-2003>, 2003.
- Zhang, L., Vet, R., O'Brien, J., Mihele, C., Liang, Z., and Wiebe, A.: Dry deposition of individual nitrogen species at eight Canadian rural sites, *J. Geophys. Res.*, 114, D02301, <https://doi.org/10.1029/2008JD010640>, 2009.
- Zhang, Q., Chang, M., Zhou, S., Chen, W., Wang, X., Liao, W., Dai, J., and Wu, Z.: Evaluate dry deposition velocity of the nitrogen oxides using Noah-MP physics ensemble simulations for the Dinghushan Forest, Southern China, *Asia-Pac. J. Atmos. Sci.*, 53, 519–536, 2017.
- Zhao, Y., Zhang, L., Chen, Y., Liu, X., Xu, W., Pan, Y., and Duan, L.: Atmospheric nitrogen deposition to China: A model analysis on nitrogen budget and critical load exceedance, *Atmos. Environ.*, 153, 32–40, 2017.
- Zheng, S. and Shangguan, Z.: Photosynthetic characteristics and their relationships with leaf nitrogen content and leaf mass per area in different plant functional types, *Acta Ecologica Sinica*, 1, 2134–2144, 2007.
- Zhong, B., Wang, X., Ye, L., Ma, M., Jia, S., Chen, W., Yan, F., Wen, Z., and Padmaja, K.: Meteorological variations impeded the benefits of recent  $\text{NO}_x$  mitigation in reducing atmospheric nitrate deposition in the Pearl River Delta region, Southeast China, *Environ. Pollut.*, 266, 115076, <https://doi.org/10.1016/j.envpol.2020.115076>, 2020.